7^{th} *International Conference on* Hydroelasticity in Marine Technology
Split, Croatia, September 16^{th}-19^{th} *2015*

Hydroelastic perspectives of ocean wave/sea ice connectivity II

Fabien Montiel[1,*] and Vernon A. Squire[1]

[1] Department of Mathematics and Statistics, University of Otago, Dunedin, New Zealand

Abstract. An idealised model of sea ice breakup in the marginal ice zone is proposed, which accounts for the two-dimensional character of ice floes in the field. Simulations of multiple scattering by large arrays of circular compliant ice floes are performed. Estimates of the likelihood and location of floe breakup are obtained by computing the principal strain over the surface of the floes. It is found that multiple scattering influences the likelihood of breakup but not its location.

Key words: *Sea ice; principal strain; floe breakup; multiple scattering*

1. Introduction

The Arctic ice cover is rapidly disappearing in summer in response to globally rising temperatures. The total surface area of open water in the Arctic Ocean is increasing as a result, so longer fetches exist which assist the generation of more energetic ocean waves [1]. Ocean waves further help the destruction of the ice cover, as they break it up as a result of hydroelastic effects, to create the marginal ice zone (MIZ) at the interface between the open ocean and the interior pack ice [2]. The MIZ consists of large arrays of ice floes of moderate sizes, where ocean waves experience conservative scattering effects as well as dissipative processes [3, 4], and constantly reshape its morphology through additional breakup.

A model of wave interaction with sea ice in the MIZ has recently been assimilated in a large scale ice/ocean model of the Arctic Ocean, and includes a parameterization of ice floe breakup [5, 6]. The model consists of one horizontal dimension however, so wave energy is bound to travel in a single direction, and the ice floe breakup model is based one dimensional thin elastic beam theory. Such floe breakup models have received much attention in the last 30 years and a general overview of this research area is presented in the companion paper Part I [7].

Two-dimensional models of wave/sea ice interactions have been much less studied, and have focused on scattering only. Unrealistic assumptions of spatial periodicity in the array are generally made [8]. A technique was recently

*Correspondence to: fmontiel@maths.otago.ac.nz

devised by the authors to include randomness in the two-dimensional scattering model [9, 10], allowing us to simulate realistic directional wave fields through random arrays of ice floes, as in the MIZ. Including ice floe breakup in such two-dimensional models remains an important challenge.

In this paper, we perform numerical simulations of our two-dimensional scattering model to determine the conditions under which floe breakup occurs in the MIZ. We assess the likelihood of breakup of a floe by calculating the maximum principal strain over the surface of the floe. Results are obtained for different configurations and a range of wave periods.

2. Scattering model

2.1. Preliminaries

We consider the scattering of surface gravity waves by a large finite array of N_f compliant circular ice floes, floating at the surface of a fluid domain with infinite horizontal extent and constant depth h. Cartesian coordinates $\mathbf{x} = (x, y, z)$ are used to locate points in the fluid, such that the planes $z = 0$ and $z = -h$ coincide with the free surface at rest and the flat seabed, respectively.

Assuming potential incompressible flow and time-harmonic motion, the fluid velocity is expressed as $(\nabla, \partial_z)\left\{(g/\mathrm{i}\omega)\phi(x, y, z)\,\mathrm{e}^{-\mathrm{i}\omega t}\right\}$, where $\nabla = (\partial_x, \partial_y)$, g is acceleration due to gravity and ω is the radian frequency. The fluid motion is then fully characterised by the complex-valued (reduced) velocity potential ϕ, which satisfies Laplace's equation

$$\left(\nabla^2 + \partial_z^2\right)\phi = 0 \tag{1}$$

everywhere in the fluid. The potential is also constrained by boundary conditions at the sea bed ($z = -h$)

$$\partial_z\phi = 0 \tag{2}$$

and at the free surface ($z = 0$ not covered by ice floes)

$$\partial_z\phi = \alpha\phi, \tag{3}$$

where $\alpha = \omega^2/g$ is the deep water wavenumber.

The ice floes are modelled as circular thin elastic plates with radius a and uniform thickness D. It can then be shown (see, e.g., [11]) that the potential satisfies the boundary condition

$$\left(\beta\nabla^4 + 1 - \alpha d\right)\partial_z\phi = \alpha\phi, \tag{4}$$

on the underside of each ice floe, $z = -d$, where $d = (\rho/\rho_0)D$ is the Archimedean draught with $\rho \approx 922.5\,\mathrm{kg\,m^{-3}}$ and $\rho_0 \approx 1025\,\mathrm{kg\,m^{-3}}$ the density of sea ice and sea water, respectively. We have also introduced the stiffness parameter $\beta = ED^3/12(1-\nu^2)\rho_0 g$, where $E \approx 6 \times 10^9\,\mathrm{Pa}$ is an effective Young's modulus for sea ice and $\nu \approx 0.3$ is Poisson's ratio. The solution method described here

can easily accommodate ice floes with different sizes and properties but in this paper we do not investigate this possibility.

Free edge conditions are further imposed, which are more conveniently expressed in local polar coordinates (r, θ) with origin at the centre of each floe (such that $\theta = 0$ defines the positive x direction). Vanishing bending moment and shear stress at $r = a$ then yield

$$\left[r^2\nabla^2_{r,\theta} - (1-\nu)\left(r\partial_r + \partial^2_\theta\right)\right]\partial_z\phi = 0 \tag{5a}$$

and

$$\left[r^3\partial_r\nabla^2_{r,\theta} + (1-\nu)\left(r\partial_r - 1\right)\partial^2_\theta\right]\partial_z\phi = 0. \tag{5b}$$

The hydroelastic system considered here is forced by a directional wave field travelling in the positive x direction. It is characterised by a superposition of plane waves with amplitudes $A^{\mathrm{In}}(\tau)$ that depend continuously on the angle of propagation τ (with respect to the x-axis), and its potential ϕ^{In} can be expressed as

$$\phi^{\mathrm{In}}(x,y,z) = \xi_0(z)\int_{-\pi/2}^{\pi/2} A^{\mathrm{In}}(\tau)\,\mathrm{e}^{\,\mathrm{i}k_0(x\cos\tau + y\sin\tau)}\,\mathrm{d}\tau, \tag{6}$$

where $\xi_0(z) = \cosh k_0(z+h)/\cosh k_0 h$ with k_0 the propagating open water wavenumber. Note that a unidirectional wave forcing at angle $\tau = \tau_0$ can be simulated by setting $A^{\mathrm{In}}(\tau) = \delta(\tau - \tau_0)$, where δ denotes the Delta function.

In response to scattering by the array of ice floes, reflected and transmitted fields are generated so that the far field can be written in the form

$$\phi(x,y,z) = \phi^{\mathrm{In}}(x,y,z) + \xi_0(z)\int_{-\pi/2}^{\pi/2} A^{\mathrm{R}}(\tau)\,\mathrm{e}^{\,\mathrm{i}k_0(-x\cos\tau + y\sin\tau)}\,\mathrm{d}\tau, \tag{7a}$$

as $x \to -\infty$ and

$$\phi(x,y,z) = \xi_0(z)\int_{-\pi/2}^{\pi/2} A^{\mathrm{T}}(\tau)\,\mathrm{e}^{\,\mathrm{i}k_0(x\cos\tau + y\sin\tau)}\,\mathrm{d}\tau, \tag{7b}$$

as $x \to \infty$. The reflected and transmitted directional amplitude functions $A^{\mathrm{R}}(\tau)$ and $A^{\mathrm{T}}(\tau)$ are unknowns of the problem.

2.2. Single floe scattering

The wave field around and below each floe is sought in cylindrical coordinates, so polar harmonic expansions are used to represent the potential. Specifically, the wave field around a floe j, $1 \le j \le N_f$, with local polar coordinates (r_j, θ_j) is decomposed into incoming and scattered components, i.e. $\phi = \phi_I^{(j)} + \phi_S^{(j)}$. These are expressed in general form as

$$\phi_I^{(j)}(r_j,\theta_j,z) \approx \sum_{m=0}^{M}\xi_m(z)\sum_{n=-N}^{N} a_{m,n}^{(j)}\mathrm{J}_n(k_m r_j)\,\mathrm{e}^{\,\mathrm{i}n\theta_j} \tag{8a}$$

and

$$\phi_S^{(j)}(r_j,\theta_j,z) \approx \sum_{m=0}^{M} \xi_m(z) \sum_{n=-N}^{N} b_{m,n}^{(j)} \mathrm{H}_n(k_m r_j)\, \mathrm{e}^{\,\mathrm{i}n\theta_j} \tag{8b}$$

valid for $r_j > a$. The potential under the floe is further given by

$$\phi_F^{(j)}(r_j,\theta_j,z) \approx \sum_{m=-2}^{M} \psi_m(z) \sum_{n=-N}^{N} c_{m,n}^{(j)} \mathrm{J}_n(\kappa_m r_j)\, \mathrm{e}^{\,\mathrm{i}n\theta_j} \tag{8c}$$

for $r_j < a$. In the expansions given above, J_n and H_n denote the Bessel and Hankel function of the first kind of order n, respectively, and the infinite sums have been truncated for the computations. We have introduced the vertical eigenfunction $\xi_m(z) = \cosh k_m(z+h)/\cosh k_m h$, $m \geq 0$, and $\psi_m(z) = \cosh \kappa_m(z+h)/\cosh \kappa_m(h-d)$, $m \geq -2$, which characterise the motion of the fluid in the vertical direction in open water and ice-covered regions, respectively. The quantities k_m, $m \geq 0$, are solutions k of the finite depth open water dispersion relation

$$k \tanh kh = \alpha,$$

with k_0 the positive real root corresponding to a propagating mode and k_m, $m \geq 1$, the purely imaginary roots corresponding to evanescent modes. Analogously, the quantities κ_m, $m \geq -2$, are solutions κ of the finite depth plate-covered dispersion relation

$$(\beta\kappa^4 + 1 - \alpha d)\kappa \tanh \kappa(h-d) = -\alpha,$$

with κ_0 the positive real root corresponding to a propagating mode, κ_m, $m \geq 1$, the purely imaginary roots corresponding to evanescent modes, and κ_{-i}, $i = 1, 2$, the complex roots with positive imaginary part which characterise damped travelling flexural gravity modes.

An eigenfunction matching method was devised by [11] for solving the single floe scattering problem for each floe j. The solution is obtained in the form of two linear matrix mappings

$$\mathbf{b}^{(j)} = \mathbf{S}_j^{\mathrm{ext}} \mathbf{a}^{(j)} \quad \text{and} \quad \mathbf{c}^{(j)} = \mathbf{S}_j^{\mathrm{in}} \mathbf{a}^{(j)}, \tag{9}$$

where $\mathbf{a}^{(j)}$, $\mathbf{b}^{(j)}$ and $\mathbf{c}^{(j)}$ are vectors containing the amplitudes $a_{m,n}^{(j)}$, $b_{m,n}^{(j)}$ and $c_{m,n}^{(j)}$, respectively. The matrices $\mathbf{S}_j^{\mathrm{ext}}$ and $\mathbf{S}_j^{\mathrm{in}}$ are commonly referred to as the exterior and interior diffraction transfer matrices of floe j.

2.3. Multiple scattering

A solution to the multiple scattering problem, where interactions between all the floes are considered, can be obtained using a direct self-consistent method (see [11]). The method was originally presented for wave interaction with multiple rigid structures by [12] and for thin-elastic plates by [13]. It consists of

expressing the incoming field on each floe j as the superposition of the ambient forcing field and the exterior scattered field from all the other floes, i.e.

$$\phi_I^{(j)} = \phi^{\mathrm{In}} + \sum_{p=1,\, p\neq j}^{N_f} \phi_S^{(p)}$$

for all j. The scattered fields $\phi_S^{(p)}$ are then converted to incoming field components on floe j using Graf's addition theorem, which then yields a system of equations for the unknown scattered field amplitudes $b_{m,n}^{(j)}$ for all floes j (see [11] for details). Direct inversion of the system is computationally manageable for $\mathrm{O}\,(100)$ floes only, which restricts significantly the range of applicability of the method for large scale multiple scattering problems.

A method has been devised to solve the multiple scattering problem considered here for large arrays, i.e. typically $\mathrm{O}\left(10^3\text{–}10^4\right)$ floes. The method is described in detail for a canonical acoustic problem in [10], so we only give a brief outline here.

1. Cluster the array of floes into N_s slab regions parallel to the y-axis, so each slab q is bounded by $x = x_{q-1}$ and $x = x_q$, and contains a smaller number of floes.

2. Express the wave field at each interface $x = x_q$, $0 \leq q \leq N_s$, as an integral of plane wave components travelling in all directions plus evanescent wave components, i.e. $\phi = \phi_q^+ + \phi_q^-$ with

$$\phi_q^{\pm}(x, y, z) = \xi_0(z) \int_\Gamma A_q^{\pm}\, \mathrm{e}^{\,\mathrm{i}k_0(\pm(x-x_q)\cos\chi + y\sin\chi)}\, \mathrm{d}\chi, \tag{10}$$

   where Γ runs from $-\pi/2 + \mathrm{i}\infty$ to $\pi/2 - \mathrm{i}\infty$ through the origin.

3. Map incident directional amplitude functions $A_{q-1}^+(\chi)$ and $A_q^-(\chi)$ to scattered directional amplitude functions $A_{q-1}^-(\chi)$ and $A_q^+(\chi)$ using the direct method described above and an integral representation of Hankel functions (see [9, 10] for the details). In discretised form, we obtain

$$\mathbf{A}_{q-1}^- = \mathfrak{R}_q^+ \mathbf{A}_{q-1}^+ + \mathfrak{T}_q^- \mathbf{A}_q^- \quad \text{and} \quad \mathbf{A}_q^+ = \mathfrak{T}_q^+ \mathbf{A}_{q-1}^+ + \mathfrak{R}_q^- \mathbf{A}_q^-, \tag{11}$$

   where $\mathfrak{R}_q^{\pm}$ and $\mathfrak{T}_q^{\pm}$ are matrices characterising reflection/transmission by the slab.

4. Solve for the unknown vectors of directional amplitudes $\mathbf{A}_q^{\pm}$ using an iterative S-matrix method (see, e.g., [14]).

The plane wave expansions (10) can then be used as forcing term in each slab and can therefore be converted as incoming waves in the form of (8a) (after some algebra). The local exterior and interior scattered fields (8b) and (8c) in each slab, are then obtained using (9).

3. Principal Strain in ice floes

In this paper, we seek to understand the conditions under which ice floes may break. The breaking criterion for ice floes is usually given in terms of the strain as discussed in the companion paper [7]. As our ice floe model is two-dimensional, the relevant measure for the strain used to compare with a given breaking strain criterion is not obvious. Here, we use the maximum value of the largest principal strain (out of the two calculated at each point) over the surface of a floe. The principal strains are the eigenvalues of Cauchy's strain tensor, such that the corresponding eigenvectors define directions in which shear strains vanish.

Under plane strain conditions, the strain tensor in a floe with local polar coordinates (r,θ) reduces to

$$\underline{\underline{E}}(r,\theta) = \frac{h}{2}\begin{pmatrix} \varepsilon_{rr} & \varepsilon_{r\theta} \\ \varepsilon_{r\theta} & \varepsilon_{\theta\theta} \end{pmatrix}, \tag{12}$$

where

$$\varepsilon_{rr} = \partial_r^2 w, \quad \varepsilon_{\theta\theta} = \frac{1}{r^2}\partial_\theta^2 w + \frac{1}{r}\partial_r w \quad \text{and} \quad \varepsilon_{r\theta} = \frac{1}{r}\partial_{r\theta}^2 w - \frac{1}{r^2}\partial_\theta w. \tag{13}$$

These expressions can be found in [15], noting the presence of a typographical error in the shear term $\varepsilon_{r\theta}$.

The quantity $w = w(r_j,\theta_j)$ refers to the vertical displacement of ice floe j and can be expressed in terms of the velocity potential at the ice/fluid interface using the kinematic condition $w = (1/\alpha)\partial_z\phi_F^{(j)}$ at $z=-d$. Using (8c) for floe j, we then obtain

$$\varepsilon_{rr} = \frac{1}{\alpha}\sum_{m=-2}^{M}\psi_m'(-d)\sum_{n=-N}^{N}\frac{\kappa_m^2}{4}c_{m,n}^{(j)}\left(\mathrm{J}_{n-2}^{(m,j)} - 2\mathrm{J}_n^{(m,j)} + \mathrm{J}_{n+2}^{(m,j)}\right)\mathrm{e}^{\mathrm{i}n\theta_j}, \tag{14a}$$

$$\varepsilon_{\theta\theta} = -\frac{1}{\alpha}\sum_{m=-2}^{M}\psi_m'(-d)\sum_{n=-N}^{N}\frac{\kappa_m}{2r_j}c_{m,n}^{(j)}\left((n-1)\mathrm{J}_{n-1}^{(m,j)} + (n+1)\mathrm{J}_{n+1}^{(m,j)}\right)\mathrm{e}^{\mathrm{i}n\theta_j} \tag{14b}$$

and

$$\varepsilon_{r\theta} = \frac{1}{\alpha}\sum_{m=-2}^{M}\psi_m'(-d)\sum_{n=-N}^{N}\frac{\mathrm{i}\kappa_m}{2r_j}c_{m,n}^{(j)}\left((n-1)\mathrm{J}_{n-1}^{(m,j)} - (n+1)\mathrm{J}_{n+1}^{(m,j)}\right)\mathrm{e}^{\mathrm{i}n\theta_j}, \tag{14c}$$

where $\mathrm{J}_l^{(m,j)} = \mathrm{J}_l(\kappa_m r_j)$, $-N \le l \le N$. Note that (14b) and (14c) are undefined at the origin. Using the asymptotic behaviour of Bessel functions for small arguments (see [16]), we derive

$$\varepsilon_{\theta\theta} \underset{r_j\to 0}{\sim} -\frac{1}{\alpha}\sum_{m=-2}^{M}\psi_m'(-d)\frac{\kappa_m^2}{4}\left(c_{m,-2}^{(j)}\mathrm{e}^{-2\,\mathrm{i}\theta_j} + 2c_{m,0}^{(j)} + c_{m,2}^{(j)}\mathrm{e}^{2\,\mathrm{i}\theta_j}\right) \tag{15a}$$

and

$$\varepsilon_{r\theta} \underset{r_j \to 0}{\sim} \frac{1}{\alpha} \sum_{m=-2}^{M} \psi'_m(-d) \frac{\mathrm{i}\kappa_m^2}{4} \left(c_{m,2}^{(j)} \, \mathrm{e}^{2\,\mathrm{i}\theta_j} - c_{m,-2}^{(j)} \, \mathrm{e}^{-2\,\mathrm{i}\theta_j} \right) \tag{15b}$$

In practice, we estimate the two principal strains at the nodes of a polar grid with 6 radii (from origin to edge) and 12 angles, and only keep the maximum value over all estimates. We denote this value by ε_m. We conjecture that the location of the maximum principal strain over the surface of the floe is where the floe is most likely to break. Measurements of breaking strain for sea ice in the field are sparse. Using strain gauges [17] found that breakup occurs for strain values between 4.4×10^{-5} and 8.5×10^{-5}. Estimations of breaking strain are discussed at length in the companion paper [7]. In the following, we use $\varepsilon_c = 5 \times 10^{-5}$ as the critical value for the breaking strain. This value will be used for comparison with our model predictions.

4. Results

In this section, we seek to determine (i) the effect of multiple scattering on maximum strain experienced by the floes and (ii) the influence of wave coherence on this quantity. We perform simulations in an idealised setting to conduct this investigation. The water depth is set to $h = 200\,\mathrm{m}$.

Consider an array composed of N_s slabs, containing P floes each. Each slab has width $W = 250\,\mathrm{m}$ and the floes in a slab are randomly perturbed from a regular arrangement with centre-to-centre spacing 250 m in the y direction, symmetric with respect to the x-axis. When not perturbed, the array therefore resembles a rectangular regular grating of ice floes. All floes are identical with radius $a = 100\,\mathrm{m}$ and thickness $D = 1\,\mathrm{m}$. The location of each floe is randomly perturbed from its mean position by $\pm 25\,\mathrm{m}$ maximum in both x and y directions (to avoid collisions between floes).

The forcing wave field ϕ^{In} is parameterized by its directional amplitude function $A^{\mathrm{In}}(\tau)$. Here we set $A^{\mathrm{In}}(\tau) = (\sqrt{(2/\pi)} \cos\tau) \exp(\,\mathrm{i}\varphi(\tau))$, $-\pi/2 \leq \tau \leq \pi/2$, which corresponds to a standard normalised cosine squared directional wave spectrum. The exponential term is a random phase term with $\varphi(\tau)$ uniformly distributed between 0 and 2π. This allows us to simulate incoherent directional wave forcing, as usually observed in the open ocean. Alternatively, we can set $\phi(\tau) = 0$ to simulate a coherent wave forcing (i.e. with phase interactions).

We analyse the response of a single floe first (i.e. $N_s = 1$ and $P = 1$) over the range of wave periods $T = 5$–$20\,\mathrm{s}$. For each wave period considered, the maximum principal strain ϵ_m is estimated as the average over 100 random realisations of the array and the wave field (for the incoherent case). Figure 1(a,b) shows the maximum principal strain ε_m for the incoherent and coherent directional wave forcing, respectively. The breaking strain ϵ_c is also shown on the plots. Error bars estimate the standard error for each data point. We observe similar qualitative behaviours for coherent and incoherent forcing, as ϵ_m reaches a maximum at $T \approx 8$–$9\,\mathrm{s}$. Quantitatively, there is a major difference, as ϵ_m is one

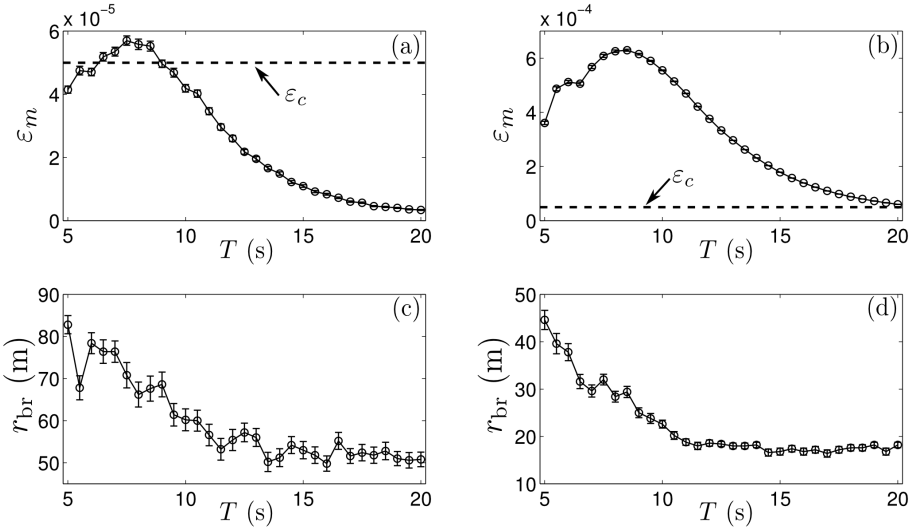

Figure 1 (a, b) Ensemble average of the maximum principal strain for a single floe under incoherent and coherent directional wave forcing. (c, d) Average distance from the floe centre where breaking is most likely to occur.

order of magnitude higher for coherent forcing than incoherent forcing. Phase interactions therefore lead to more bending and a higher probability of breakup, as we have $\varepsilon_m > \varepsilon_c$ for all T in the coherent forcing case. For incoherent wave forcing, we have $\varepsilon_m < \varepsilon_c$ except near the maximum point mentioned earlier, so that the floe is unlikely to break except close to the resonant frequency. It is therefore probable that coherent hydroelastic models of wave/sea ice interactions will overestimate the likelihood of ice breakup.

We also analyse the location on the ice floe surface where ε_m is calculated, in order to infer the most probable point where the breakup will occur (if at all). It was found that the maximum strain is measured on average on the negative x-axis, i.e. $\theta = \pi$, likely due to the symmetry of the problem under consideration. For each wave period we estimate the average of the distance to the origin where breakup most likely takes place, $r_{\rm br}$. This quantity is plotted in Figure 1(c,d). Different results are obtained for coherent and incoherent forcings. In the former case, $r_{\rm br}$ decreases from $\approx 40\,$m down to $\approx 20\,$m between $T = 5$ and $10\,$s, and then plateaus for longer waves. For the incoherent forcing, breakup will most likely occur closer to the edge (on average), as $r_{\rm br}$ decreases from 70–80 m at $T = 5\,$s to 40–50 m at $T = 20\,$s.

Now consider a single slab containing $P = 51$ floes randomly distributed in the slab under the constraints described earlier. Only the incoherent wave forcing is considered here, as it is more reasonable. Figure 2 shows ε_m and $r_{\rm br}$ for the range of wave periods considered. Each value is the mean of the

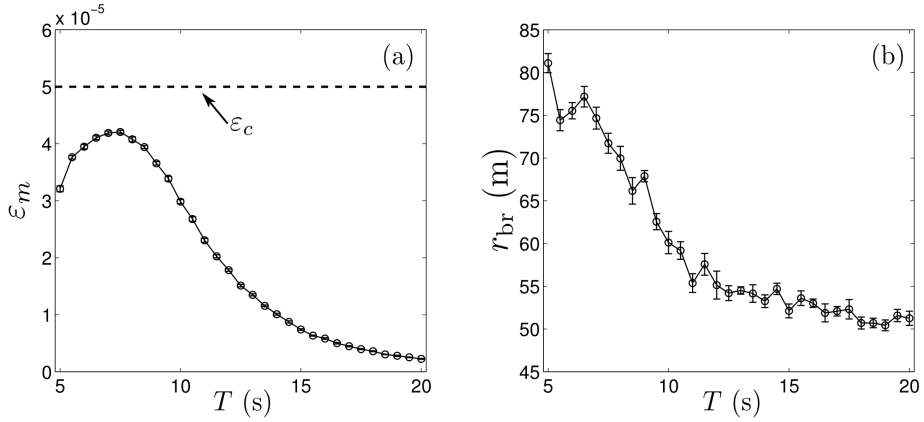

Figure 2 (a) Ensemble average of the maximum principal strain for an array of 51 floes randomly distributed in a slab. (b) Average distance from the floe centre where breaking is most likely to occur.

maximum principal strain calculated in each floe over all floes. Results are further averaged over 10 random realisations of the array and forcing. We observe that ε_m is now below ε_c for all wave periods, and in general is smaller than for the single floe problem. Multiple scattering effects therefore tend to lower the strain experienced by the floes on average, and consequently the probability of breakup. On the other hand, $r_{\rm br}$ looks remarkably similar to the single floe values, so multiple scattering does not influence the point where floes are most likely to break on average.

Finally, we consider a larger array composed of $N_s = 20$ slabs with $P = 51$ floes in each slab, i.e. more than 1000 floes. We want to determine how the properties of floe breakup evolve through the array, particularly with distance from the ice edge, i.e. $x = 0$. The quantities ε_m and $r_{\rm br}$ are calculated as the mean over all floes in each slab. Incoherent forcing is only considered here. Results are averaged over 10 random realisations of the array and forcing.

Figure 3 shows the evolution of ε_m through the array for four different wave periods, i.e. $T = 6,\ 9,\ 12$ and 15 s. The corresponding single slab values (see Figure 2) are also indicated. The behaviour observed is similar for all wave periods. The maximum principal strain decreases through the array, as more wave energy is attenuated (or increasingly reflected) for increasing x. The value of ε_m is higher than that of the single slab problem in the front rows but then becomes lower farther in. Multiple reflection/transmission processes between slabs therefore increase the probability of floe breakup close to the ice edge, compared to a single slab in isolation. Specifically, our model predicts floe breakup at $T = 6$ s in the first kilometre of the array, while no breakup would occur for a single slab.

The evolution of the distance to floe centre where breakup is most likely to

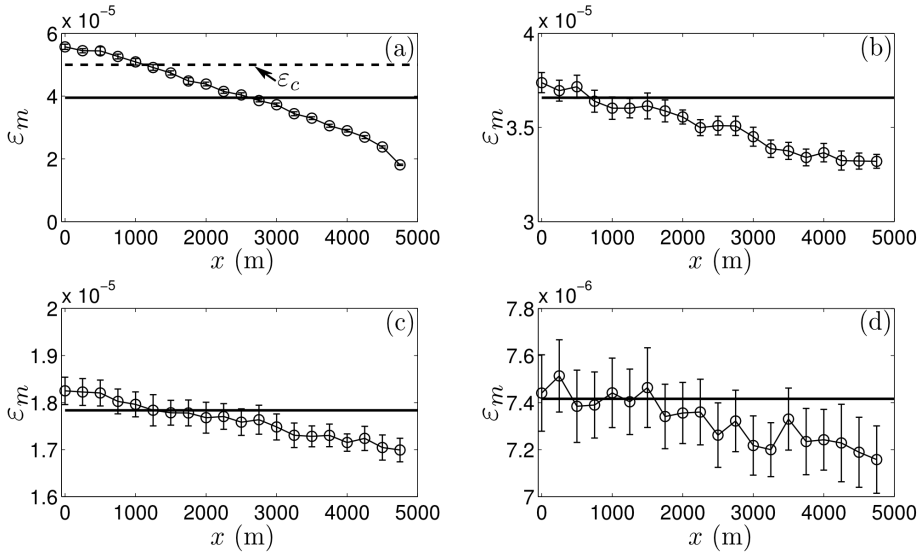

Figure 3 Average maximum principal strain in each slab for a 20-slab array plotted against x. Results are given for (a) $T = 6\,\mathrm{s}$, (b) $9\,\mathrm{s}$, (c) $12\,\mathrm{s}$ and (d) $15\,\mathrm{s}$. The corresponding single slab values are given for comparisons.

occur, i.e. r_{br}, through the array is displayed in Figure 4 for the same wave periods. We observe very little variation of r_{br} as the wave field evolves through the array and the single slab value is similar. Consequently, multiple reflection/transmission does not affect where a floe is most likely to break up on average, and this property is mainly dependent on the characteristics of the single floe.

5. Conclusion

In this paper, we described an idealised model of floe breakup for ice floes in the MIZ. We performed simulations of wave multiple scattering for an array of ice floes with random properties and a realistic incoherent directional wave forcing. The maximum principal strain is computed in each floe to determine the likelihood of floe breakup. The main findings are listed below.

- Coherent wave fields overestimate the strain experienced by ice floes by as much as one order of magnitude, compared to incoherent forcing.
- Coherence also leads to predictions of floe breakup closer to the floe centre than for incoherent wave forcing.
- Multiple scattering effects in a slab of ice floes reduces the likelihood of floe breakup on average.

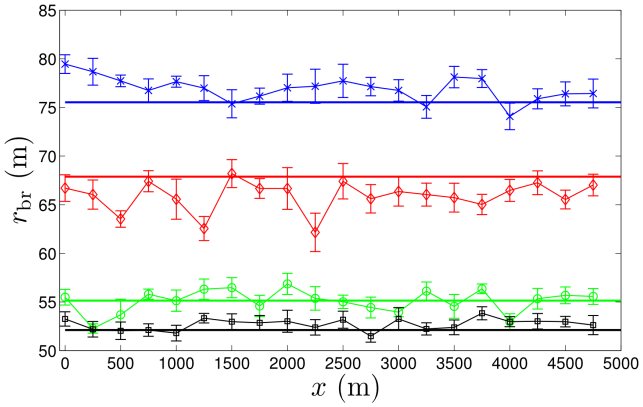

Figure 4 r_{br} plotted against x for $T = 6\,\mathrm{s}$ (blue), $9\,\mathrm{s}$ (red), $12\,\mathrm{s}$ (green) and $15\,\mathrm{s}$ (black). The corresponding single slab values are given for comparisons.

- Multiple scattering does not influence the location on the floe surface where breakup is most likely to occur.
- The probability of breakup generally decreases with distance from the ice edge, while it is enhanced close to the ice edge due to reflected wave energy from deeper into the ice cover.

The results obtained in this paper are qualitative only as breakup would strongly depend on (i) the intensity of the wave forcing, (ii) the properties of the ice floes, e.g. thickness, Young's modulus, ... and (iii) the heterogeneity of MIZ in terms of floe sizes and shapes. This is a first step, however, towards integrating a parameterization of floe breakup in two (horizontal) dimensions in large scale models, in order to improve the current one dimensional approach.

Acknowledgments

The authors acknowledge financial support from the US office of Naval Research (Award Number N00014-131-0279), the European Union (Grant FP7-Space-2013-1-SWARP-607476) and the University of Otago.

References

[1] J. Thomson and W. E. Rogers. Swell and sea in the emerging arctic ocean. *Geophys. Res. Lett.*, 41(9):3136–3140, 2014.

[2] T. Toyota, C. Haas, and T. Tamura. Size distribution and shape properties of relatively small sea-ice floes in the antarctic marginal ice zone in late winter. *Deep-Sea Res Pt. II*, 58:1182–1193, 2011.

[3] V. A. Squire, J. P. Dugan, P. Wadhams, P. J. Rottier , and A. K. Liu. Of ocean waves and sea ice. *Annu. Rev. Fluid Mech.*, 27:115–168, 1995.

[4] V. A. Squire. Of ocean waves and sea-ice revisited. *Cold Reg. Sci. Technol.*, 49:110–133, 2007.

[5] T. D. Williams, L. G. Bennetts, V. A. Squire, D. Dumont, and L. Bertino. Wave-ice interactions in the marginal ice zone. part 1: Theoretical foundations. *Ocean Model.*, 71:81–91, 2013.

[6] T. D. Williams, L. G. Bennetts, V. A. Squire, D. Dumont, and L. Bertino. Wave-ice interactions in the marginal ice zone. part 2: Numerical implementation and sensitivity studies along 1d transects of the ocean surface. *Ocean Model.*, 71:92–101, 2013.

[7] V. A Squire and F. Montiel. Hydroelastic perspectives of ocean wave/sea ice connectivity I. In *Proceedings of the 7th International Conference on Hydroelasticity in Marine Technology*, Split, Croatia, 2015.

[8] L. G. Bennetts, M. A. Peter, V. A. Squire, and M. H. Meylan. A three dimensional model of wave attenuation in the marginal ice zone. *J. Geophys. Res.*, 115:C12043, 2010.

[9] F. Montiel, V. A. Squire, and L. G. Bennetts. Reflection and transmission of ocean wave spectra by a band of randomly distributed ice floes. *Ann. Glaciol.*, 56(69):315–322, 2015.

[10] F. Montiel, V. A. Squire, and L. G. Bennetts. Evolution of directional wave spectra through finite regular and randomly perturbed arrays of scatterers. *SIAM J. Appl. Math.*, 75:630–651, 2015.

[11] F. Montiel, L. G. Bennetts, V. A. Squire, F. Bonnefoy, and P. Ferrant. Hydroelastic response of floating elastic discs to regular waves. part 2. modal analysis. *J. Fluid Mech.*, 723:629–652, 2013.

[12] H. Kagemoto and D. K. P. Yue. Interactions among multiple three-dimensional bodies in water waves: an exact algebraic method. *J. Fluid Mech.*, 166:189–209, 1986.

[13] M. A. Peter and M. H. Meylan. Infinite-depth interaction theory for arbitrary floating bodies applied to wave forcing on ice floes. *J. Fluid Mech.*, 500:145–167, 2004.

[14] D. Y. K. Ko and J. R. Sambles. Scattering matrix method for propagation of radiation in stratified media: attenuated total reflection studies of liquid crystals. *J. Opt. Soc. Am. A*, 5(11):1863–1866, 1988.

[15] M. H. Meylan and V. A. Squire. Response of a circular ice floe to ocean waves. *J. Geophys. Res.*, 101:8869–8884, 1996.

[16] M. Abramowitz and I. A. Stegun. *Handbook of Mathematical Functions*. Dover, 1970.

[17] V. A. Squire and S. Martin. A field study of the physical properties, response to swell, and subsequent fracture of a single ice floe in the winter bering sea. Technical report, Univiversity of Washington, 1980.